Proceedings of the Second International Conference on Press-in Engineering 2021, Kochi, Japan – Matsumoto et al (eds)

Vertical and diagonal pull-out experiments of flip-type ground anchors embedded in dry sand in plane-strain condition

S. Yoshida, X. Xiong & T. Matsumoto
Graduate School of Natural Science and Technology, Kanazawa University, Kanazawa, Japan

M. Yoshida
Daisho Co., Ltd., Shiga, Japan

ABSTRACT: The flip anchor is pressed or driven into the ground. The anchor head rotates to open when pull-out force acts on it. In this study, vertical and diagonal pull-out experiments of flip anchors in plane strain condition were carried out to investigate the pull-out mechanism of flip anchors. Rectangular model anchors with wire rope, which had a width of 98 mm and a breadth of 48 or 80 mm, were used. Experimental parameters were embedment depth of the anchor h, pull-out angle α and initial embedment angle of the anchor plate β. As h became deeper, the maximum pull-out force F_{max} increased. Other parameters had only a minor influence on F_{max}. Soil above the anchor head was lifted in inverted trapezoidal shape when the anchor was pulled vertically. Therefore, calculated F_{max} estimated from the vertical pull-out model of opened anchor could be applied to predict F_{max} at any α.

1 INTRODUCTION

1.1 *Flip-type earth anchors*

Flip-type earth (ground) anchors (hereinafter referred to as "flip anchor") (Figure 1) are effective means for reinforcing slopes against slope failures. A decisive difference from soil nails and ground anchor, which are also used for slope reinforcement, is that flip anchors do not require grouting for the installation. The flip anchors have been applied also for supporting tower structures against strong winds and can be applied even under water to support floating structures (Anchoring Rope and Rigging Pty Ltd. 2020b). The flip anchors are versatile anchors because the equipment for construction is small-scale and do not require drilling, cement and curing period.

Figure 2 Shows an installation procedure of the flip anchors. The flip anchors are driven or pressed into the ground with its anchor head closed (Figure 2a). When pull-out force acts on the anchor, the anchor head rotates to open so that soil pressure sufficiently acts on it (Figure 2b). Although the installation procedure of flip anchors is simple and quick, the mechanism of their pull-out resistance has not been completely understood yet.

1.2 *Review of related researches*

The behaviors of embedded plate anchors, such as square anchors, rectangular anchors, or circular anchors in sand, have been investigated in previous studies. Through mainly laboratory experiments, ground failure patterns were observed and some theoretical approaches to estimate pull-out capacity of those plate anchors have been proposed so far.

Majer (1955) proposed the frictional cylinder model (Figure 3a). The model assumes that the ground is failed in a cylindrical shape with the anchor plate as the bottom surface. The pull-out resistance is calculated from the sum of the weight of the cylindrical soil above the anchor plate and the frictional resistance of the peripheral surface of the soil cylinder.

Mors (1959) proposed the cone model (Figure 3b). The model assumes that truncated cone-shaped model consisting of failure lines extending to the ground surface at $90 + \phi$ from both edge of the anchor plate. In this model, only the weight of the soil in the truncated cone is counted to obtain the pull-out capacity.

Balla (1961) observed a failure pattern consisting of circular failure line from the edge of the anchor (Figure 3c). The circular line meets the ground surface at an angle of approximately $45° - \phi/2$. The pull-out resistance is calculated from the weight of the soil and the friction along the circular failure lines based on the Kötter's equation.

The accuracy of the theoretical formulas derived from these three models depends largely on the ratio of anchor embedment depth h to anchor diameter d (or width B) h/d. For example, Mors' model (Figure 3b) tends to overestimate the pull-out

DOI: 10.1201/9781003215226-57

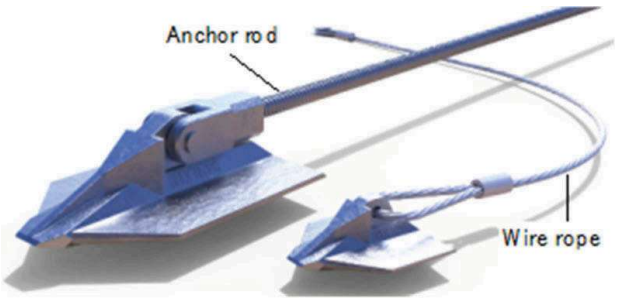

Figure 1. Examples of flip anchor (Anchoring Rope and Rigging Pty Ltd. 2020a).

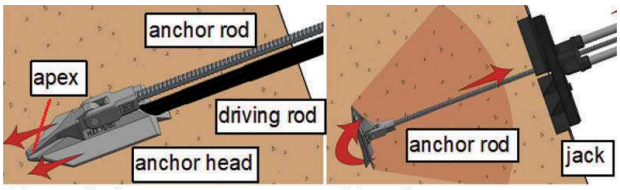

Figure 2. Installation procedure of flip anchor.

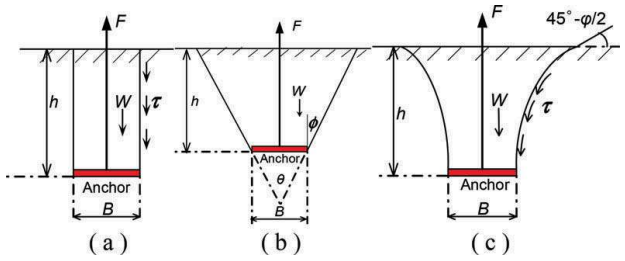

Figure 3. Typical ground failure patterns.

resistance of deep anchors where the slip line does not reach the ground surface. Balla's method (Figure 3c) also overestimates pullout capacity of deep anchor for a similar reason.

Baker & Konder (1966) pointed out the necessity of applying different formulas depending on the ratio h/d from their results of model experiment and field experiment. h/d of 6 was proposed as the border to distinguish between a shallow anchor and a deep anchor. For shallow anchors, Meyerhof & Adams (1968) proposed a practical theory to estimate pull-out capacity. For deep anchors, Vesić (1971, 1975) did the same. However, it is still difficult to determine h/d that distinguishes between shallow and deep anchors depending on various conditions. Tagaya et al. (1988) dealt with the depth that distinguishes between the shallow and the deep anchor as critical depth D_{fcr}. Tagaya et al. (1988) organized and introduced the theoretical formulas and conducted centrifugal experiment and finite element analysis on pull-out capacity of circular and rectangular plate anchors.

Many other researches have been conducted in consideration of other parameters, such as ground density or anchor shape (Das & Seeley 1975, Murray & Geddes 1987, Sutherland 1988, Ilamparuthi et al. 2002). Particle image velocimetry (PIV) or digital image correlation (DIC) methods, which analyze the photographs taken during the experiments of push-up test on a trap door (Tanaka & Sakai 1987) or pull-out test of anchors (Liu et al. 2012), were applied in order to observe ground failure patterns.

A lot of studies have been conducted also using the numerical analysis. Sakai & Tanaka (2007) conducted the FEM analysis on development of shear band for a circulate anchor pulled out in sand ground. Furthermore, some numerical analyses compared the results obtained from past empirical formulas and experiments with the results of numerical analysis (Merifield & Sloan 2006).

It has been reported based on small-scale model experiments that the scale effect exists (Ovensen 1979, Neely et al. 1973, Tanaka & Sakai 1993). It is known that this effect can be avoided by centrifugal experiments (Dickin 1988).

However, those studies focused on embedded horizontal or vertical plate anchors. In other words, the pull-out mechanism of the flip anchor, which is pressed or driven into the ground and rotates and resists in the soil when pull-out force acts, has not been treated in the past studies. Niroumand & Kassim (2013) conducted a pull-out experiment using an actual flip anchor. However, like other studies on plate anchors, the flip anchor was embedded horizontally before being pulled out. It is because that the pull-out test focused on the effects of its irregular shape on the pull-out resistance.

1.3 *Objectives of this research*

The behaviors of flip anchors have not been investigated sufficiently, as mentioned above. Therefore, in this study, a series of two-dimensional (plane strain condition) pull-out experiments of model flip anchors in dry sand are carried out to obtain the pull-out resistance and to observe the corresponding ground failure patterns. Based on the experimental results, a simplified ground failure model and a simple calculation method for the pull-out resistance of flip anchor under plane strain condition are proposed.

2 OUTLINE OF THE EXPERIMENTS

2.1 *Model ground*

A transparent acrylic box having a length of 800 mm, a height of 500 mm and a width of 98 mm was used as a soil box for the model ground (Photo 1).

Dry silica sand #3 was used for the model ground. Physical properties of the sand are listed in Table 1. Model ground was prepared in 10 layers of 50 mm thick. Relative density D_r of the model ground was adjusted to be about 80 % (dry density ρ_d = 1.512 ton/m^3) by tapping the sand of each layer.

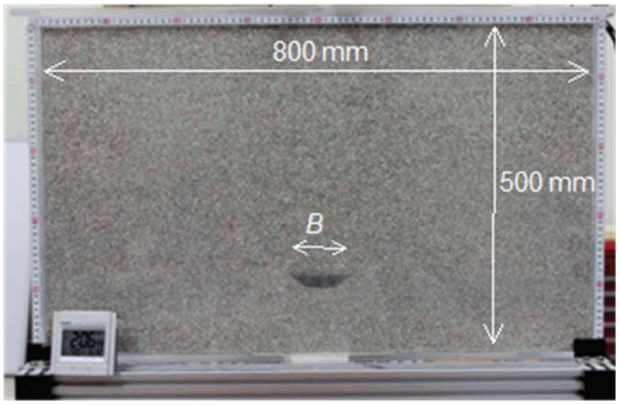

Photo 1. Model ground in a transparent soil box.

Table 1. Physical properties of silica sand #3.

Property	Value
Density of soil particles, ρ_s (ton/m^3)	2.632
Max. dry density, $\rho_{d\,max}$ (ton/m^3)	1.567
Min. dry density, $\rho_{d\,min}$ (ton/m^3)	1.325
Max. void ratio, e_{max}	0.987
Min. void ratio, e_{min}	0.679

Internal friction angle $\phi' = 42°$ was obtained from direct shear tests of the sand with $D_r = 80\%$.

2.2 *Model anchors*

The model anchor used for the experiment is shown in Figure 4. A steel plate having a breadth B of 48 or 80 mm, a width of 98 mm and a thickness of 5 mm. Wires are attached to eye bolts on the anchor for pulling the anchor. The wires can move on the ring of the eye bolt freely, so that the anchor can rotate to open when pulled.

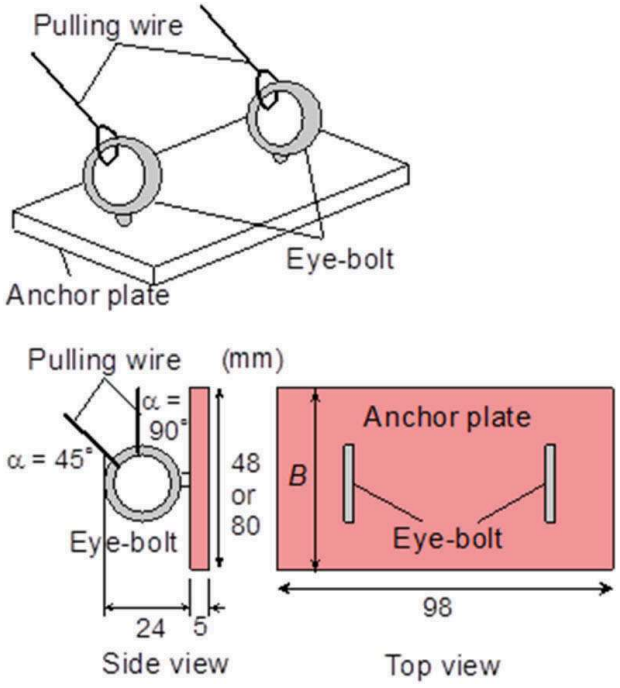

Figure 4. Dimensions of model flip anchor.

2.3 *Experimental cases and procedure*

Figure 5 shows a set-up for the pull-out experiments of anchors. A model anchor with a pulling wire is embedded at a given embedment depth during the preparation of the model ground. A winch for pulling the wire was set on a loading frame. A load cell (LC) to measure pull-out force F was set between the winch and the pulling wire. Pull-out displacement w of the anchor was measured with an encoder (ENC). Five earth pressure gages (EP) were set to a side wall of the box to measure lateral earth pressures at different depths.

The transparent soil box makes particle image velocimetry (PIV) analysis possible. Photos were taken from the front side at an interval of 2 seconds to observe the behavior of the sand particles. The photos were processed using a software named Trackpy (Trackpy Contributors, 2019) to obtain the traces of the soil particles during the pull-out experiment.

Table 2 lists all the cases of pull-out experiments. Figures 6 and 7 show conditions of pull-out experiments. The model anchor was embedded in the model ground at a given embedment depth h. The embedment depth h was varied as 100, 200, 300 and 400 mm, and the breadth of anchor B was 48 or 80 mm. The pull-out angles α was set at 45 or 90 degrees. Under the condition of $\alpha = 90°$, the anchor

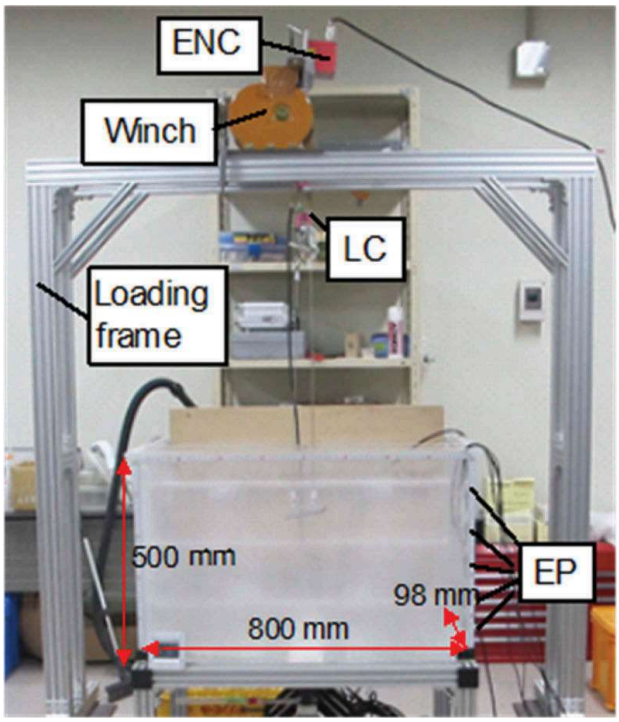

Figure 5. Experimental set-up for pull-out experiment.

Table 2. Experimental cases.

Case	B (mm)	Opened or Closed	h (mm)	α(deg)	β
01	48	Opened	400	90	0
02	48	Closed	400	90	-90
03	48	Opened	400	90	0
04	48	Opened	300	90	0
05	48	Opened	200	90	0
06	48	Opened	100	90	0
13	80	Opened	100	90	0
14	80	Opened	200	90	0
15	80	Opened	300	90	0
16	80	Opened	400	90	0
17	48	Closed	400	90	-90
18	48	Closed	300	90	-90
19	48	Closed	200	90	-90
20	48	Closed	100	90	-90
21	48	Closed	100	90	-90
22	48	Closed	200	90	-90
23	48	Closed	300	90	-90
24	48	Closed	400	90	-90
25	48	Opened	100	45	45
26	48	Opened	200	45	45
27	48	Opened	300	45	45
28	48	Opened	400	45	45
29	48	Closed	100	45	-45
30	48	Closed	200	45	-45
31	48	Closed	300	45	-45
32	48	Closed	400	45	-45
33	48	Closed	100	45	90
34	48	Closed	200	45	90
35	48	Closed	300	45	90
36	48	Closed	400	45	90

was pulled out vertically, and at 45 degrees, it was pulled out diagonally. β is embedment angle of anchor plate (see Figure 6). There were five types of experiments with different combinations of α and β, as shown in Figure 7. They can be broadly divided into Opened or Closed conditions to the pull-out direction.

A total of 30 cases of experiments were conducted as listed in Table 2.

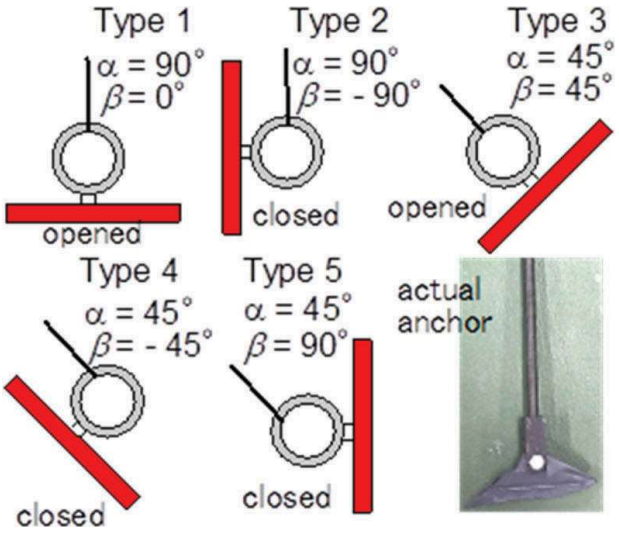

Figure 7. Experimental types.

3 RESULTS OF THE EXPERIMENTS

3.1 *Pull-out force vs. pull-out displacement*

(a) Influence of h

Figures 8 and 9 show comparisons of relationships between pull-out force F and pull-out displacement w of Opened (β = 0°) anchors under different embedment depths h. As expected, F became larger when the anchors were embedded deeper in the ground. F of the larger anchor (B = 80 mm) was larger than F of the smaller anchor (B = 48 mm) at the same h. The projected area A of the larger anchor was about 1.7 times A of the smaller anchor. However, F of the larger anchor at every h is about 1.3

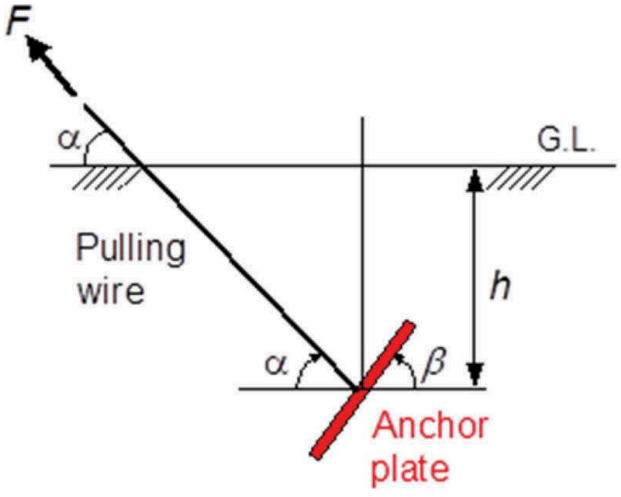

Figure 6. Definitions of experimental parameters.

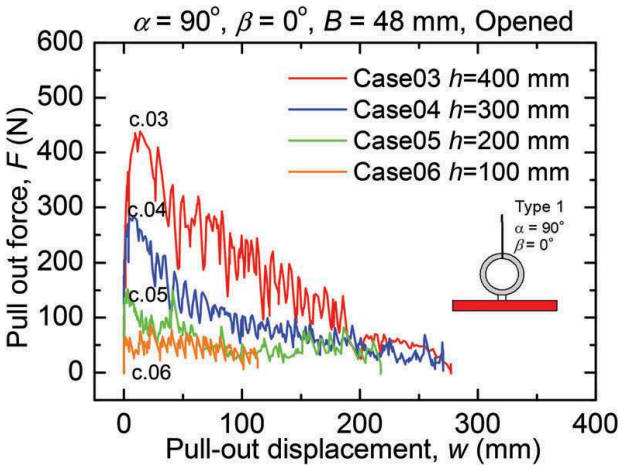

Figure 8. F vs. w of Type 1 with different h (B = 48 mm).

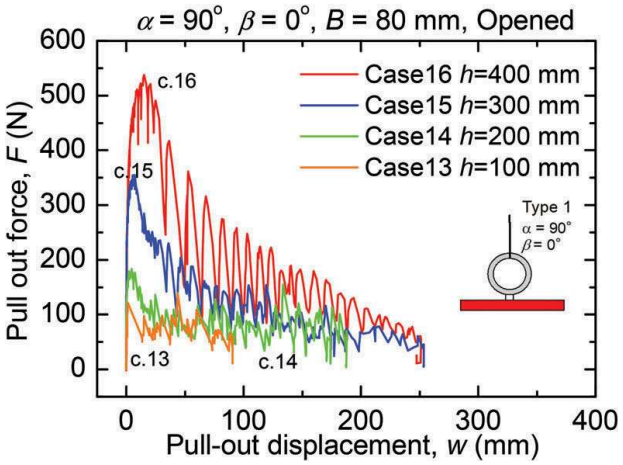

Figure 9. F vs. w of Type 1 with different h (B = 80 mm).

times larger than F of the smaller anchor That is, F did not increase as much as the ratio of A.

Figure 10 is the comparison of maximum pull-out force F_{max} of each Opened anchor when pulled vertically (α = 90°). F_{max} of the both anchors increased with h. F_{max} of the larger anchor was larger than F_{max} of the smaller anchor at any h. However, as mentioned above, F_{max} did not increase as much as the ratio of the projected area A of each anchor.

Figure 11 is the comparison of maximum pull-out stress p_{max} (= F_{max}/A) of each anchor. Contrary to F_{max}, p_{max} became larger as A became smaller. From the results of Figures 10 and 11, it can be seen that p_{max} is affected by other factors besides overburden pressure.

(b) Influences of α and β

Figures 12-15 show comparisons of F vs. w of Opened (β = 0°) and Closed (β = -90°) anchors under different h. Regardless of pull-out angle α and embedment angle of anchor plate β, F became larger when the anchors were embedded deeper in the ground. F vs. w of anchors (Types 2 to 5) showed almost similar tendency to that of Type 1 anchor (Figure 8).

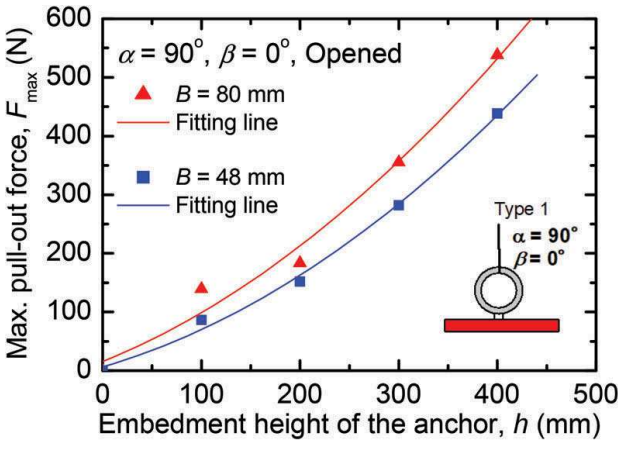

Figure 10. F_{max} vs. h of Type 1.

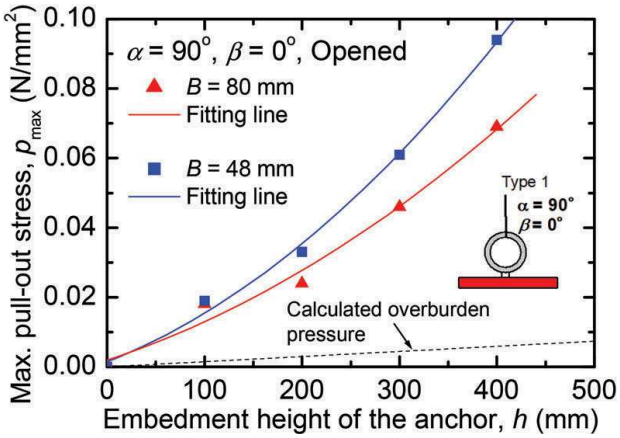

Figure 11. P_{max} vs. h of Type 1.

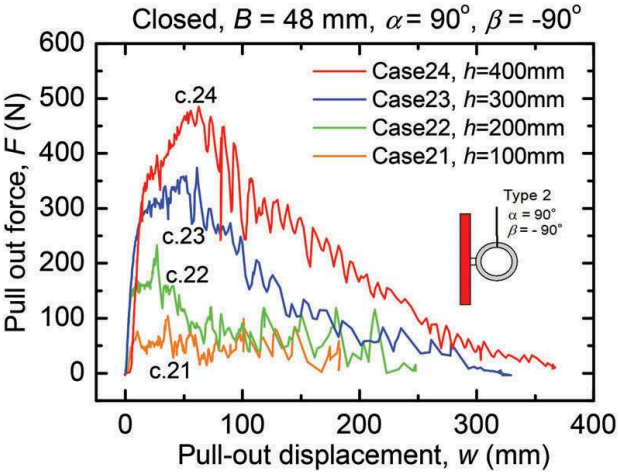

Figure 12. F vs. w of Type 2 with different h.

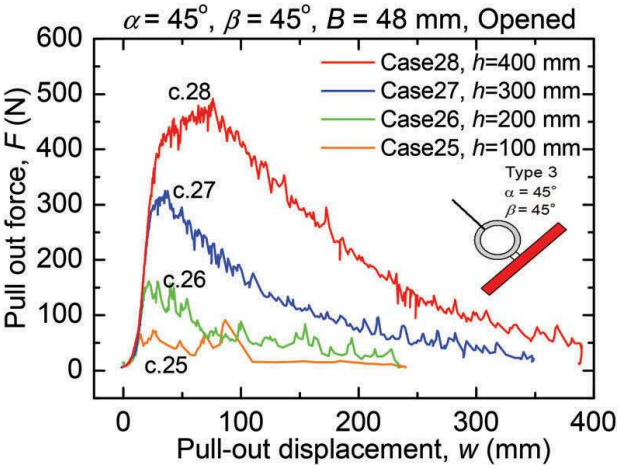

Figure 13. F vs. w of Type 3 with different h.

Figure 16 shows the relationships between F and w of Opened and Closed anchors embedded at the same h were pulled out in the vertical direction (α= 90°). F_{max} of Closed anchor (Type 2) was larger than that of Opened anchor (Type 1). However, larger w was necessary to attain F_{max} in Closed anchor.

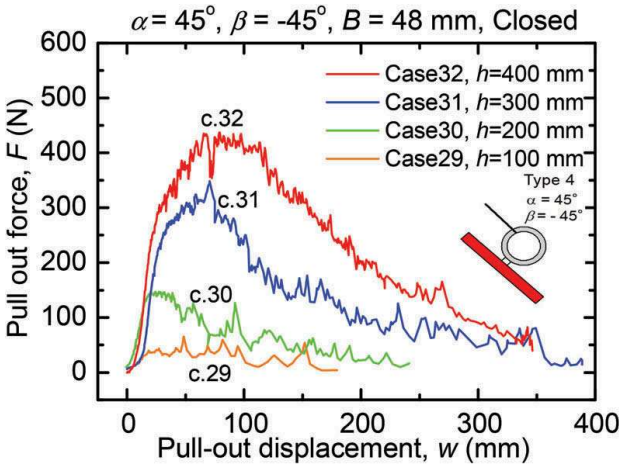

Figure 14. F vs. w of Type 4 with different h.

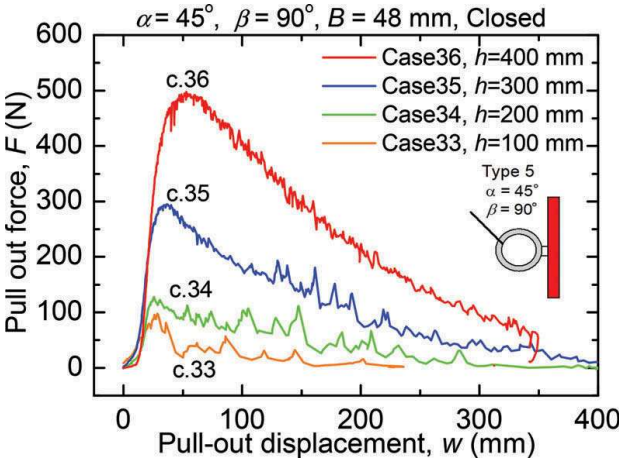

Figure 15. F vs. w of Type 5 with different h.

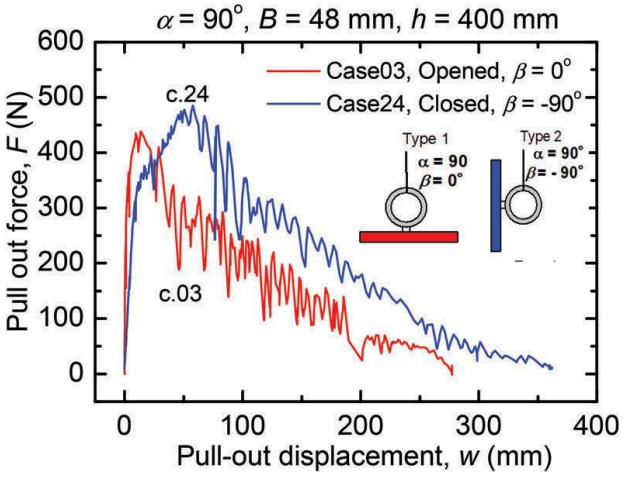

Figure 16. F vs. w of Type 1 and Type 2 with $\alpha = 90°$.

Figure 17 is F vs. w of the anchors with different β and the same h, when they were pulled out in the diagonal direction ($\alpha = 45°$). F_{max} of Type 5 was almost equal to that of Type 3. F_{max} of Type 4 was about 80% of that of Type 3. There were some differences in the amount of w at F_{max}. For example,

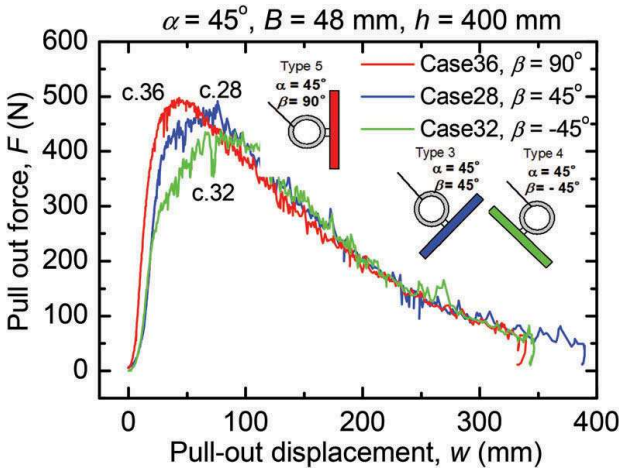

Figure 17. F vs. w of Types 3, 4 and 5 with $\alpha = 45°$.

w of Types 3 and 4 at F_{max} were larger than that of Type 5. In general, β had little effect on F vs. w.

Figure 18 shows F vs. w of Opened anchors under different pull-out angles (α = 90° or 45°). It was found again that αas well as β did not significantly affect F_{max}.

Figure 19 is a similar comparison to Figure 18 for Closed anchors. Same as Opened anchors (Figure 18), α as well as β did not significantly affect F_{max}.

It may be concluded from the results of Figures 16-19 that F_{max} of various anchor types are comparable to F_{max} of Type 1 (Opened anchor pulled out in the vertical direction). Hence, the ground failure in Type 1 is discussed and a simple method of estimating F_{max} is proposed next.

3.2 *Modelling of ground failure*

In this research, the PIV analysis was also carried out. Figure 20 shows (a) photo of ground deformation with displacement vectors and (b) zoom-up of the traces of the sand particles until pull-out displacement of the anchor w reached 15.1 mm at F_{max}

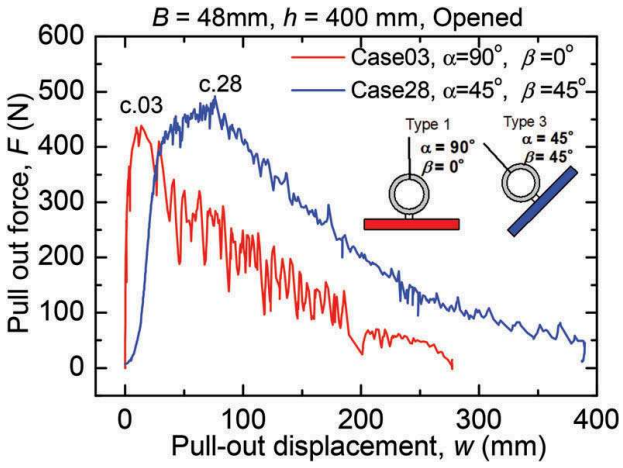

Figure 18. F vs. w of Type 1 and Type 3 with different combinations of α and β.

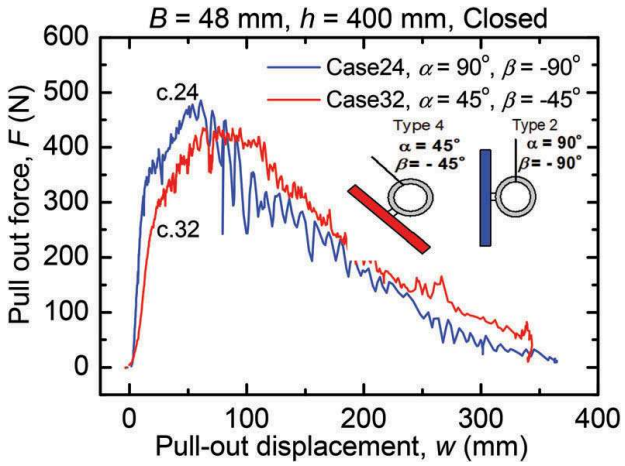

Figure 19. F vs. w of Type 2 and Type 4 with different combinations of α and β.

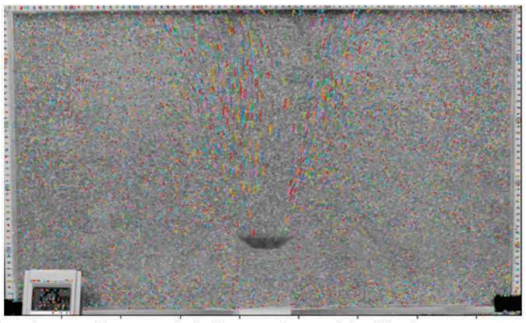

(a) Photo of ground deformation with displacement vectors

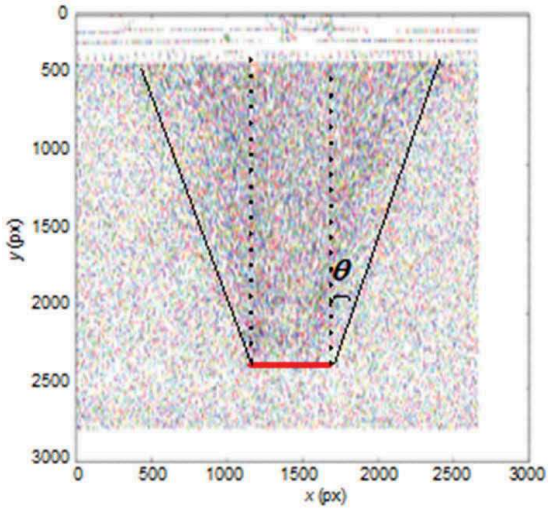

(b) Displacement vectors of ground (Enlarged)

Figure 20. Photo of ground deformation and displacement vectors at F_{max} (Case 16: B = 80 mm, h/B=5).

= 538 N in Case 16. An inverted trapezoidal failure pattern was clearly observed.

Figure 21 Shows similar results of the PIV analysis of Case 1 (w = 13.0 mm at F_{max} = 438 N). An inverted trapezoidal failure pattern was observed clearly again.

It is seen from Figures 20 and 21 that the ground failure patterns were similar regardless of anchor width B. The angle of the slip lines from the vertical

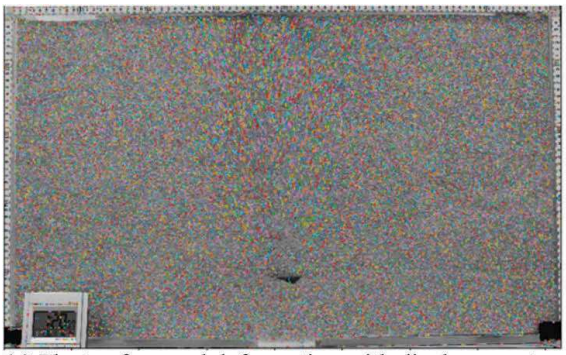

(a) Photo of ground deformation with displacement vectors

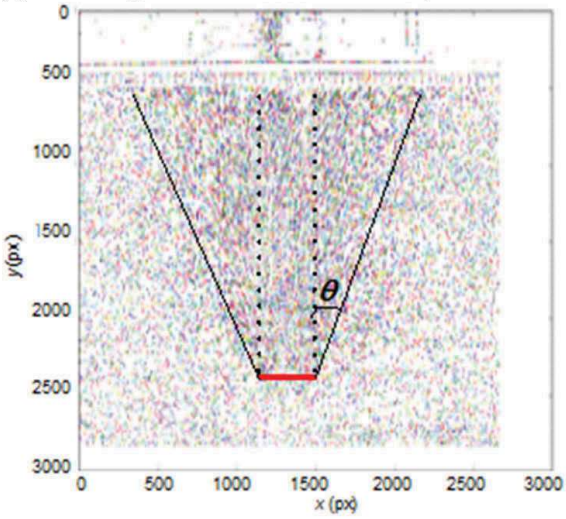

(b) Displacement vectors of ground (Enlarged)

Figure 21. Photo of ground deformation and displacement vectors at F_{max} (Case 1: B = 48 mm, h/B=8.3).

direction θ was 21° in both cases. And the θ observed in all the vertical pull-out experiments ranged from 20° to 22°. The average was approximately θ = 21°. It is close to an angle of $45° - \phi'/2(\phi' = 42°)$.

The ground failure patterns observed in this study could be simply modelled as Figure 22. It is similar to Mors' model (Figure 3b), although θ is assumed to be equal to ϕ' in Mors' model. In Mors' model (Figure 3b), the pull-out resistance F_{max} is calculated from only the weight of the soil W of the inverted truncated cone above the anchor plate.

On the other hand, in the two-dimensional model proposed in this study (Figure 22), the pull-out resistance F_{max} is calculated from the weight W of the inverted trapezoidal soil wedge and the vertical component of the shear resistance T acting along the slip lines, as Eq. (1).

$$F_{max} = 2(W_1 + W_2 + T\cos\theta) \qquad (1)$$

3.3 *Estimate of pull-out resistance of plate anchors*

Figure 23 shows measured F_{max} vs. calculated F_{max} for each size of the anchors when pulled-out vertically. In the calculations, $\phi' = 42°$ obtained from the direct shear tests of the sand was used. As mentioned

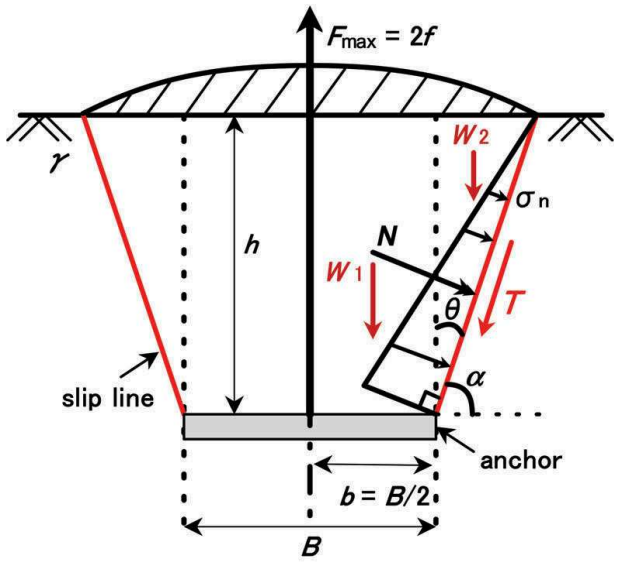

h: embedment depth of anchor
γ: unit weight of soil
W_1: $W_1 = \gamma \times b \times h \times D$ (D: depth of anchor)
W_2: $W_2 = \gamma \times h \times h \tan\theta \times 1/2 \times D$
θ: angle of slip line
N: normal force acting on slip line
T: shear force acting along slip line, $T = N \tan\phi'$
B: width of anchor
b: $b = B/2$
f: force acting on the half of anchor
$f = W_1 + W_2 + T\cos\theta$
F_{max}: total force acting on anchor, $F = 2f$
σ_n: $(1+K_0)\sigma_v'/2 + (1-K_0)(\sigma_v'/2)\cos 2\alpha$
σ_v': effective vertical stress
K_0: coefficient of earth pressure at rest

Figure 22. Two-dimensional model of ground failure.

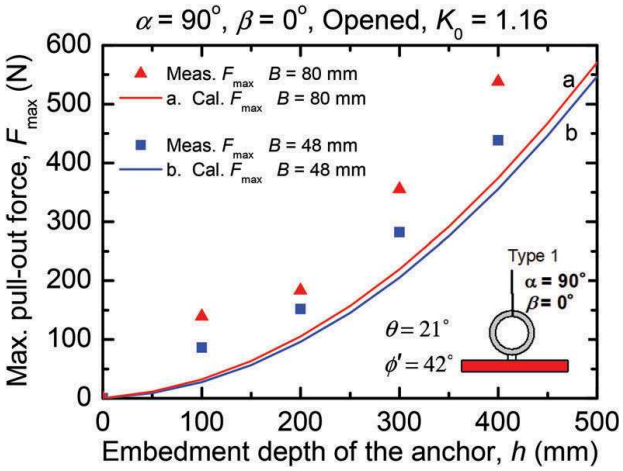

Figure 23. Relationship of measured and calculated F_{max}.

in Figure 5, five earth pressure gauges were set on the side wall of the soil box. After the preparation of the model ground, an average value of K_0 = 1.16 was obtained. This relatively high K_0 value may be caused by a tapping method used for the ground preparation. The calculated F_{max} qualitatively agreed well with the measured results.

As mentioned earlier, through the pull-out experiments, the pull-out angle α and the embedment angle of anchor plate β did not significantly affect the value of F_{max}. Hence, the simplest vertical pull-out model of horizontal anchor (Type 1) could be applied to the estimation of other conditions (Types 2 to 5). The proposed model could be applied also to flip anchors, because Closed anchors were included in Types 2 to 5.

It is noticed that the maximum h/B in the pull-out experiments was 8.3 (h = 400 mm/B = 48 mm). Hence, the proposed model could be applied to shallow anchors, whose h/B are smaller than 8.

4 CONCLUSIONS

In this study, pull-out experiments of model flip-type anchors in dry sand ground under plane strain (two-dimensional) condition were carried out. Main experimental parameters of the pull-out experiments were embedment depth h, breadth of the anchors B, pull-out angle α and embedment angle of anchor plate β.

Main findings from the experiments are summarized as:

(1) The maximum pull-out force F_{max} increased as h increased.
(2) F_{max} of the larger anchor (B = 80 mm) was larger than F_{max} of the smaller anchor (B = 48 mm) at the same h.
(3) Contrary to the tendency of F_{max}, maximum stress p_{max} (= F_{max}/A) became larger as B became smaller.
(4) α, aswell as β did not significantly affect F_{max}. That is, F_{max} of anchors with various α and β is approximated by F_{max} of Opened plate anchor under the vertical pull-out condition.
(5) The ground failure pattern in the pull-out experiments was simply modelled, based on the observations of ground deformation. F_{max} calculated from the proposed model qualitatively agreed well with measured F_{max} of each pull-out condition.

The proposed two-dimensional ground failure model for shallow anchors could be extended to three-dimensional conditions.

REFERENCES

Anchoring Rope and Rigging Pty Ltd. 2020. https://hulkearthanchors.com, 2020a.

Anchoring Rope and Rigging Pty Ltd. 2020. https://www.arandr.com.au/articles/projects, 2020b.

Balla, A. 1961. The resistance to breaking-out of mushroom foundations for pylons. *Proceedings of the 5th international conference on Soil Mechanics and Foundation Engineering*: 569–576.

Baker, W. H. & Konder, R. L. 1966. Pullout load capacity of a circular earth anchor buried in sand. *Highway Research Record* 108: 1–10.

Das, B. M. & Seeley, G. R. 1975. Breakout resistance of shallow horizontal anchors. *Journal of the Geotechnical Engineering Division* 101 (9): 999–1003.

Dickin, E.A. 1988. Uplift behavior of horizontal anchor plates in sand. *Journal of Geotechnical Engineering* 114 (11): 1300–1317.

Ilamparuthi, K., Dickin, E.A. and Muthukrisnalah, K. 2002. Experimental investigation of the uplift behaviour of circular plate anchors embedded in sand. *Canadian geotechnical journal* 39 (31): 648–664.

Liu, J., Liu M. & Zhu, Z. 2012. Sand Deformation around an Uplift Plate Anchor. *Journal of Geotechnical and Geoenvironmental Engineering* 138 (6): 728–737.

Majer, J. 1955. Zur berechnung von zugfundamenten. *Osterreichister, Bauzeitschift* 10 (5): 85–90.

Merifield, R.S. & Sloan S.W. 2006. The ultimate pullout capacity of anchors in frictional soils. *Canadian Geotechnical Journal* 43: 852–868.

Meyerhof, G. G. & Adams, J. I. 1968. The ultimate uplift capacity of foundations. *Canadian Geotechnical Journal*, 5 (41): 225–244.

Mors, H. 1959. Das Verhalten von Mastgruendungen bei Zugbeanspruchung, *Bautechnik* 39 (10): 367–378.

Murray, E.J. & Geddes, J.D. 1987. Uplift of anchor plates in sand. *Journal of Geotechnical Engineering* 113 (3): 202–215.

Neely, W. J., Stuart, J.C. and Graham, J. 1973. Failure loads of vertical anchor plates in sand. *Journal of Soil Mechanics and Foundations Div., ASCE* 99 (9):669–685.

Niroumand, H. & Kassim, K.A. 2013. Pullout capacity of irregular shape anchor in sand. *Measurement* 46 (10): 3872–3882.

Ovensen, N. K. 1979. The use of physical models in design: the scaling law relationship. *Proceeding of 7th European Conference on Soil Mechanics and Foundation Engineering* 4: 318–323.

Sakai, T. & Tanaka, T. 2007. Experimental and Numerical Study of Uplift Behavior of Shallow Circular Anchor in Two-Layered Sand. *Journal of Geotechnical and Geoenvironmental Engineering* 133 (4): 469–477.

Sutherland, H.B. 1988. Uplift resistance of soils. *Géotechnique*, 38 (4): 493–516.

Tagaya, K., Scott, R.F. and Aboshi, H. 1988. Pullout resistance of buried anchor in sand. *Soils and foundations* 28 (3): 114–30.

Tanaka, T. & Sakai, T. 1987. A trap-door problem in granular materials: Model test and FEA, *Journal of Irrigation Engineering and Rural Planning* 11: 8–23.

Tanaka, T. & Sakai, T. 1993. Progressive failure and scale effect of trap-door problems with granular materials. *Soils and Foundations* 33 (1): 11–22.

Trackpy Contributors, 2019. https://soft-matter.github.io/trackpy/v0.3.2/

Vesić, A. S. 1971. Breakout Resistance of Objects Embedded in Ocean Bottom. *Journal of the Soil Mechanics and Foundations Division* 97 (9): 1183–1205.

Vesić, A. S. 1975. Principles of Pile Foundation Design, *Soil mechanics series* 38.